THE JOURNAL OF PHYSICAL CHEMISTRY B

ARTICLE

pubs.acs.org/JPCB

Fingerprints for Structural Defects in Poly(thienylene vinylene) (PTV): A Joint Theoretical−Experimental NMR Study on Model Molecules

H. Diliën,[†] L. Marin,[†] E. Botek,[§] B. Champagne,[§] V. Lemaur,[∥] D. Beljonne,[∥] R. Lazzaroni,[∥] T. J. Cleij,[†] W. Maes,[†] L. Lutsen,[‡] D. Vanderzande,[†,‡] and P. J. Adriaensens*[,†]

[†]Institute for Materials Research (IMO) − Chemistry Division, Hasselt University, Universitaire Campus, Building D, B-3590 Diepenbeek, Belgium

[‡]IMEC, Division IMOMEC, Universitaire Campus, Wetenschapspark 1, B-3590 Diepenbeek, Belgium

[§]Laboratoire de Chimie Théorique, Facultés Universitaires Notre-Dame de la Paix (FUNDP), Rue de Bruxelles 61, 5000 Namur, Belgium

[∥]Service de Chimie des Matériaux Nouveaux, Université de Mons-UMONS, Place du Parc 20, B-7000 Mons, Belgium

Supporting Information

ABSTRACT: In the field of plastic electronics, low band gap conjugated polymers like poly(thienylene vinylene) (PTV) and its derivatives are a promising class of materials that can be obtained with high molecular weight via the so-called dithiocarbamate precursor route. We have performed a joint experimental−theoretical study of the full NMR chemical shift assignment in a series of thiophene-based model compounds, which aims at (i) benchmarking the quantum-chemical calculations against experiments, (ii) identifying the signature of possible structural defects that can appear during the polymerization of PTV's, namely head-to-head and tail-to-tail defects, and (iii) defining a criterion regarding regioregularity.

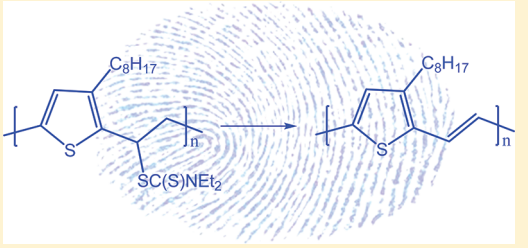

INTRODUCTION

Various classes of conjugated polymers have been studied as components of the active layer in devices,[1−6] in particular for photovoltaic applications. To overcome the mismatch between the absorbance window of the semiconducting polymer and the solar spectrum, low band gap materials have been investigated thoroughly.[7−13] Poly(thienylene vinylene) (PTV)-based polymers absorb light of longer wavelengths with respect to "classical" polyalkylthiophenes and are therefore considered as promising materials.[14−19] The synthesis of PTV derivatives is, however, very challenging. Two different strategies are applied, i.e., condensation reactions[20,21] that generally lead to low molecular weight polymers and precursor routes.[22−31] It has been presented earlier that the dithiocarbamate precursor route is the only protocol that allows for the creation of stable monomers for polymerization.[32−36] In recent work, the precursor route toward poly(3-octylthienylene vinylene) (O-PTV) has been explored extensively by NMR spectroscopy to identify and quantify the polymer end groups and possible structural defects due to, e.g., head-to-head or tail-to-tail monomer additions during the polymerization process.[37] For that purpose, ^{13}C-labeled vinylene carbons were introduced into the polymer chains. Solubility in several organic solvents was ensured by the long octyl side chains. Unfortunately, limited information has been reported so far concerning the complete assignment of proton and carbon chemical shifts of these defects. Furthermore, according to literature data, poly(thienylene vinylene) derivatives that are prepared via a condensation reaction are 100% regioregular. It has been claimed that the degree of regioregularity can be determined by ^{1}H and ^{13}C NMR spectroscopy.[21,38]

Here, we perform a joint experimental−theoretical NMR study on relevant model compounds for the polymers and identify fingerprints for structural defects, end-groups, and regioregularity. The results also provide useful information regarding the prediction of NMR chemical shifts for this class of materials, for which experimental data are rather scarce.

EXPERIMENTAL SECTION

General. All of the commercially available chemicals were purchased from Acros or Sigma-Aldrich and were used without further purification unless stated otherwise. Tetrahydrofuran (THF) and diethyl ether used in the synthesis were dried by distillation from sodium/benzophenone. All reactions were carried out under inert atmosphere.

Techniques. ^{1}H and ^{13}C NMR spectra were recorded on a Varian Inova 300 or 400 spectrometer from solutions in deuteroform (D 99.8%). The chemical shifts were calibrated by means of the (remaining) proton and carbon resonance signals of $CDCl_3$ (7.24 and 77.7 ppm for ^{1}H and ^{13}C, respectively). Quantitative

Received: July 13, 2011
Revised: September 6, 2011
Published: September 06, 2011

1D NMR experiments are complemented with other pulse sequences like APT (attached proton test), 2D-HETCOR (heteronuclear correlation spectroscopy), and 2D-INADEQUATE (incredible natural abundance double quantum transfer experiment). The latter is used for some compounds to assign the carbon-backbone. GC/MS analyses were carried out on TSQ-70 and Voyager mass spectrometers (Thermoquest); capillary column: Chrompack Cpsil5CB or Cpsil8CB. Fourier transform-infrared spectroscopy (FT-IR) was performed on a Perkin-Elmer Spectrum One FT-IR spectrometer (nominal resolution 4 cm^{-1}, summation of 16 scans).

Synthesis. Reference compounds **2c**, **2f**, and **2h** are commercially available. The synthesis of model and reference compounds **1b**, **1c**, **1d**, **2a**, **2b**, **2d**, and **2g** has been reported earlier.[37]

Model Compound ***1b***. ^{1}H NMR ($CDCl_3$, δ in ppm, J in Hz): 7.19 (dd, J_1 = 5.2, J_2 = 1.3, 1H), 7.06 (dd, J_1 = 5.0, J_2 = 1.3, 1H), 6.99 (dd, J_1 = 3.5, J_2 = 1.3, 1H), 6.90 (dd, J_1 = 5.2, J_2 = 3.5, 1H), 6.84 (dd, J_1 = 5.0, J_2 = 3.5, 1H), 6.81 (dd, J_1 = 3.5, J_2 = 1.3, 1H), 5.62 (dd, J_1 = 9.9, J_2 = 4.7, 1H), 4.01 (q, J = 6.9, 2H), 3.84 (dd, J_1 = 14.8, J_2 = 4.7, 1H), 3.69 (q, J = 6.9, 2H), 3.43 (dd, J_1 = 14.8, J_2 = 9.9, 1H), 1.26 (t, J = 6.9, 3H), 1.25 (t, J = 6.9, 3H).

^{13}C NMR ($CDCl_3$, δ in ppm): 194.2, 143.1, 141.3, 127.4, 127.2, 127.1, 126.9, 125.7, 124.7, 52.9, 50.0, 47.4, 38.8, 13.2, 12.3.

Model Compound ***1c***. ^{1}H NMR ($CDCl_3$, δ in ppm, J in Hz): 7.14 (dd, J_1 = 5.1, J_2 = 1.2, 2H), 6.93 (dd, J_1 = 5.1, J_2 = 3.6, 2H), 6.82 (dd, J_1 = 3.6, J_2 = 1.2, 2H), 3.21 (s, 4H).

^{13}C NMR ($CDCl_3$, δ in ppm): 144.3, 127.4, 125.3, 124.0, 32.8.

Model Compound ***1d***. ^{1}H NMR ($CDCl_3$, δ in ppm, J in Hz): 7.18 (dd, J_1 = 5.0, J_2 = 1.1, 2H), 7.06 (s, 2H), 7.04 (dd, J_1 = 3.6, J_2 = 1.1, 2H), 6.99 (dd, J_1 = 5.0, J_2 = 3.6, 2H).

^{13}C NMR ($CDCl_3$, δ in ppm): 143.0, 128.3, 126.7, 125.0, 122.1.

Reference Compound ***2a***. ^{1}H NMR ($CDCl_3$, δ in ppm, J in Hz): 7.14 (dd, J_1 = 5.1, J_2 = 1.2, 1H), 7.01 (dd, J_1 = 3.5, J_2 = 1.2, 1H), 6.88 (dd, J_1 = 5.1, J_2 = 3.5, 1H), 4.75 (s, 2H), 3.98 (q, J = 7.3, 2H), 3.65 (q, J = 7.3, 2H), 1.23 (2t, J_1 = 7.3, 6H). ^{13}C NMR ($CDCl_3$, δ in ppm): 194.4, 139.2, 127.3, 127.0, 125.6, 49.8, 47.1, 36.7, 12.8, 11.9.

Reference Compound ***2b***. ^{1}H NMR ($CDCl_3$, δ in ppm, J in Hz): 7.09 (d, J = 5.1, 1H), 6.81 (d, J_1 = 5.1, 1H), 4.67 (s, 2H), 4.01 (q, J = 7.4, 2H), 3.68 (q, J = 7.4, 2H), 2.58 (t, J = 7.7, 2H), 1.57 (p, J = 7.7, 2H), 1.36−1.21 (m, 16 H), 0.87 (t, J = 6.8, 3H).

^{13}C NMR ($CDCl_3$, δ in ppm): 195.0, 141.8, 131.0, 129.1, 124.2, 49.7, 47.1, 35.5, 32.3, 31.2, 29.9 (2X), 29.7, 28.8, 23.1, 14.6, 12.9, 12.0.

Reference Compound ***2c***. ^{1}H NMR ($CDCl_3$, δ in ppm, J in Hz): 7.19 (dd, J_1 = 5.2, J_2 = 1.2, 1H), 7.02 (dd, J_1 = 5.2, J_2 = 3.4, 1H), 6.89−6,87 (m, 1H), 2.62 (d, J = 1.2, 3H).

^{13}C NMR ($CDCl_3$, δ in ppm): 139.8, 127.3, 125.6, 123.5, 15.2.

Reference Compound ***2d***. ^{1}H NMR ($CDCl_3$, δ in ppm, J in Hz): 7.22 (dd, J_1 = 4.9, J_2 = 3.1, 1H), 6.92 (dd, J_1 = 4.9, J_2 = 1.3, 1H), 6.91 (dd, J_1 = 3.1, J_2 = 1.3, 1H), 2.61 (t, J = 7.7, 2H), 1.60 (p, J = 7.7, 2H), 1.36−1.21 (m, 10H), 0.87 (t, J = 6.4, 3H).

^{13}C NMR ($CDCl_3$, δ in ppm): 143.6, 128.7, 125.5, 120.3, 32.6, 31.3, 31.0, 30.2, 30.12, 30.06, 23.4, 14.8.

Synthesis of Reference Compound ***2e***

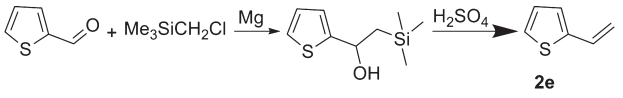

Step 1: 1-(Thiophen-2-yl)-2-(trimethylsilyl)ethanol. Chloromethyltrimethylsilane (6.1 g, 50.0 mmol) was added dropwise to a suspension of magnesium turnings (1.25 g, 50 mmol) in dry THF (150 mL), and the mixture was allowed to react under reflux conditions for 4 h. To the freshly prepared Grignard solution, cooled to −78 °C, was added dropwise thiophene-2-carbaldehyde (5.32 g, 47.5 mmol). The mixture was allowed to react for 1 h at −78 °C and then left at room temperature overnight. The reaction mixture was poured in 50 mL of cold NH_4Cl solution (10%, vol.). The organic layer was washed with H_2O and $NaHCO_3$ (10%, vol.) and dried over anhydrous Na_2SO_4, and the solvent was removed under reduced pressure. Purification of the crude product by vacuum distillation afforded the pure alcohol as a colorless oil (8.72 g, 87% yield).

^{1}H NMR ($CDCl_3$, δ in ppm, J in Hz): 7.21 (dd, J_1 = 4.9, J_2 = 1.4, 1H), 6.94 (dd, J_1 = 3.5, J_2 = 1.4, 1H), 6.91 (dd, J_1 = 4.9, J_2 = 3.5, 1H), 5.12−5.04 (m, 1H), 1.95 (d, J = 4.4, 1H), 1.30 (dd, J_1 = 7.4, J_2 = 6.0, 2H), 0.02−0.00 (m, 9H).

MS (EI, m/e): 200 (M^+).

*Step 2: Synthesis of 2-Vinylthiophene (****2e****).* Concentrated sulfuric acid (6 drops) was added to a solution of 1-(thiophen-2-yl)-2-(trimethylsilyl)ethanol (2.0 g, 10 mmol) in dry THF (10 mL), and the mixture was allowed to react under reflux for 2 h. The reaction was quenched by the addition of a cold NH_4Cl solution (10%, vol.), and the aqueous phase was extracted with diethylether. The combined organic layers were dried over anhydrous $MgSO_4$. Evaporation of the solvent under reduced pressure afforded the pure title compound **2e** in a nearly quantitative manner.

^{1}H NMR ($CDCl_3$, δ in ppm, J in Hz): 7.16 (dd, J_1 = 3.6, J_2 = 1.9, 1H), 6.95 (dd, J_1 = 3.6, J_2 = 1.9, 1H), 6.94 (t, J = 3.6, 1H), 6.81 (dd, J_1 = 10.9, J_2 = 17.5, 1H), 5.57 (d, J = 17.5, 1H), 5.14 (d, J = 10.9, 1H).

^{13}C NMR ($CDCl_3$, δ in ppm): 143.7, 130.5, 128.0, 126.5, 125.0, 113.9.

MS (EI, m/e): 110 (M^+).

Reference Compound ***2f***. ^{1}H NMR ($CDCl_3$, δ in ppm, J in Hz): 9.91 (d, J = 1.2, 1H), 7.77 (dd, J_1 = 3.9, J_2 = 1.2, 1H), 7.75 (dt, J_1 = 4.9, J_2 = 1.2, 1H), 7.20 (dd, J_1 = 4.9, J_2 = 3.9, 1H).

^{13}C NMR ($CDCl_3$, δ in ppm): 183.7, 144.6, 137.0, 135.8, 129.0.

Reference Compound ***2g***. ^{1}H NMR ($CDCl_3$, δ in ppm, J in Hz): 7.27 (dd, J_1 = 5.0, J_2 = 1.3, 1H), 7.01−7.00 (m, 1H), 6.96 (dd, J_1 = 5.0, J_2 = 3.5, 1H), 4.82 (d, J = 3.5, 2H), 1.79 (s, 1H).

^{13}C NMR ($CDCl_3$, δ in ppm): 144.2, 127.0, 125.6, 125.5, 59.3.

Reference Compound ***2h***. ^{1}H NMR ($CDCl_3$, δ in ppm, J in Hz): 12.50 (s, 1H), 7.89 (dd, J_1 = 3.8, J_2 = 1.2, 1H), 7.64 (dd, J_1 = 5.0, J_2 = 1.2, 1H), 7.13 (dd, J_1 = 5.0, J_2 = 3.8, 1H).

^{13}C NMR ($CDCl_3$, δ in ppm): 168.8, 135.8, 134.8, 133.5, 128.8.

Theoretical and Computational Section. The structures of the model compounds were optimized using density functional theory (DFT) with the B3LYP hybrid exchange-correlation functional and the 6-311G(d) basis set. For the PTV trimers, the B97-D/6-31G(d,p) method was used, since it includes a semiempirical treatment of the London dispersion forces. Then, the chemical shifts of all systems were obtained with the B3LYP functional and the 6-311+G(2d,p) basis set together with the GIAO method to ensure origin-independence, following the approach that was employed and tested recently for PVC oligomers[39,40] as well as fluoroionophores.[41,42] No attempt to use the B97-D XC functional for calculating the NMR chemical shift has been made, since there is no reason to believe it would improve over B3LYP and it is beyond the scope of this paper to assess its reliability.

Scheme 1. Polymerization of 3-Octyl-2,5,-diylbismethylene *N,N*-Diethyl Dithiocarbamate Towards O-PTV[a]

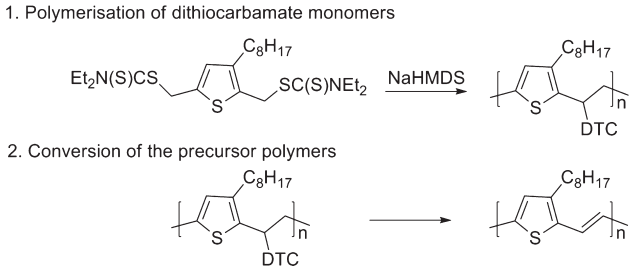

[a] DTC = DiThioCarbamate = $-SC(S)NEt_2$.

Solvent (here chloroform) effects were taken into account by using the IEFPCM approach[43] for the calculations of the chemical shifts of all compounds. In addition, solvent effects were also considered in the geometry optimizations of the PTV trimers. Based on the energies obtained at the optimization step, the most stable conformers were selected and their Maxwell–Boltzmann (MB) weights were calculated to estimate the average chemical shifts. As shown in recent works for other families of compounds, linear fits between the experimental and theoretical chemical shifts of simple compounds can be used to facilitate the interpretation of spectroscopic data of more complex systems.[39,44] So, in a preliminary step, the linear regression parameters were obtained from the NMR and theoretical data on a series of simple reference thiophene derivatives (**2a**–**2h**), and they were employed in a subsequent step to correct the calculated values for systematic errors.

RESULTS AND DISCUSSION

Possible Polymerization Defects in Precursor and Conjugated O-PTV Materials and the Corresponding Model Compounds. Scheme 1 describes the polymerization of 3-octyl-2,5-diylbismethylene *N,N*-diethyl dithiocarbamate toward O-PTV via the dithiocarbamate precursor route.[33] The first step consists of the formation of the so-called precursor polymer by normal head-to-tail addition of monomers. However, several structural defects can appear as a result of head-to-head and tail-to-tail additions (Figure 1a). In a second step, the precursor polymer is converted into the conjugated chain by means of an elimination reaction.[45] The structures of possible defects in the conjugated polymer are represented in Figure 1b. To identify the NMR chemical shifts of all of these structural units in the precursor as well as in the conjugated polymers, a joint theoretical–experimental study has been performed on a series of model compounds (Figure 1c).

In the precursor polymer, three structural units can appear which are represented by model compounds **1a**, **1b**, and **1c**. Two of them are described both theoretically and experimentally, namely molecule **1b** representing the normal head-to-tail linkage and molecule **1c** mimicking a structural defect associated with head-to-head monomer addition. The synthesis of these two model compounds was reported earlier.[37] The NMR characterization of these model compounds is described below. The third possible unit in the precursor polymer is a tail-to-tail defect (**1a**), for which the chemical shifts have been predicted solely from theoretical calculations.

Six different structural units can be encountered in the O-PTV conjugated polymer. Structural unit **1b** might still be present as a

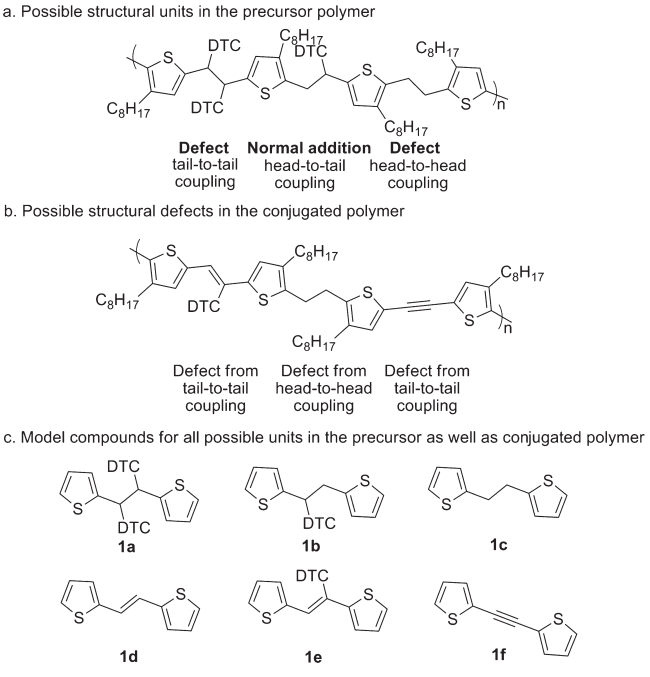

Figure 1. Possible structural defects in O-PTV.

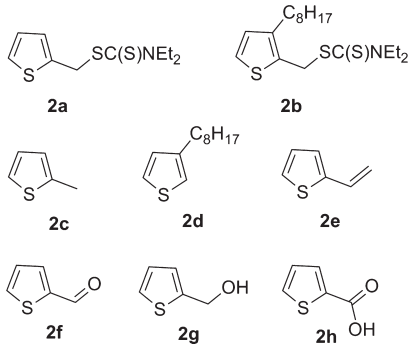

Figure 2. Reference compounds for DFT theoretical modeling.

result of incomplete conversion of normal head-to-tail units toward a trans double bond (**1d**). Model compound **1d** has been synthesized and the NMR shifts have been determined. Structures **1a** and **1e** might both be found in the conjugated polymer due to incomplete elimination of a tail-to-tail defect. Elimination of both dithiocarbamate groups of a tail-to-tail defect results in the formation of triple bonds as in **1f**. As for **1a**, **1e** and **1f** were only investigated by theoretical modeling.

Reference Calibration Molecules for DFT Calculations of NMR Chemical Shifts. To assess the accuracy of the DFT calculations, several previously synthesized reference compounds (**2a**–**2h**)[37] have been fully characterized with ^{1}H and ^{13}C NMR techniques (Figure 2). Based on this chemical shift information, the chemical shifts of all model compounds, in particular **1a**, **1e**, and **1f**, have been computed (vide infra).

Experimental NMR Characterization of the Reference Compounds and Model Compounds 1b–d. The next paragraph describes the assignment of the proton and carbon NMR chemical shifts of the reference and model compounds. The atomic numbering scheme of the thiophene derivatives is shown in Figure 3.

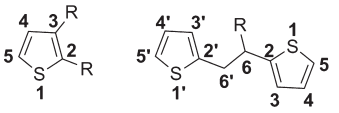

Figure 3. Numbering of the thiophene structures.

Figure 4. Assignment of the chemical shifts of thiophene-2-carbaldehyde (**2f**).

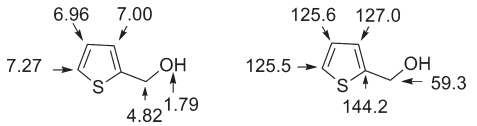

Figure 5. Assignment of the chemical shift of 2-thiophenemethanol (**2g**).

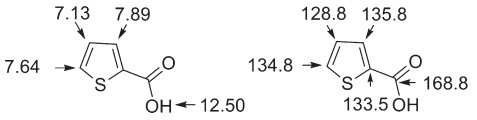

Figure 6. Assignment of the chemical shift of 2-thiophenecarboxylic acid (**2h**).

The chemical shift assignment of the carbon atoms of thiophene-2-carbaldehyde (**2f**; Figure 4) has been accomplished by means of 2D-INADEQUATE. Starting from the aldehyde carbon atom at 183.7 ppm, the carbon resonances of C2, C3, C4 and C5 can be assigned to the signals at 144.6, 137.0, 129.0, and 135.8 ppm, respectively. The corresponding proton shifts were assigned by HETCOR, i.e., H-3 appears at 7.77 ppm (dd, J_1 = 3.9, J_2 = 1.2, 1H), H-5 at 7.75 ppm (dt, J_1 = 4.9, J_2 = 1.2, 1H), and H-4 at 7.20 ppm (dd, J_1 = 4.9, J_2 = 3.9, 1H).

The chemical shifts of 2-thiophenemethanol (**2g**; Figure 5) were assigned by means of selective proton decoupling. First the proton coupling between H-3 and the two benzylic protons was removed by selective decoupling of the benzylic protons at 4.82 ppm (d, J = 3.5 Hz, 2H). In this way H-3 could be assigned to the signal at 7.00 ppm (m, 1H). The other protons are assigned based on their coupling constants. H-4 appears at 6.96 ppm - (dd, J_1 = 5.0 Hz, J_2 = 3.5 Hz, 1H) and H-5 is assigned to the signal at 7.27 ppm (dd, J_1 = 5.0 Hz, J_2 = 1.3 Hz, 1H). The carbon shifts have been assigned by APT and HETCOR.

The signals of 2-thiophene carboxylic acid (**2h**; Figure 6) were assigned by means of 2D-INADEQUATE. Starting from the carboxylic carbon atom at 168.8 ppm, the carbon resonances of C2, C3, C4, and C5 can be assigned to the signals at 133.5, 135.8, 128.8, and 134.8 ppm, respectively. The corresponding proton shifts were again assigned by HETCOR, i.e., H-3 can be attributed to 7.89 ppm (dd, J_1 = 3.8, J_2 = 1.2, 1H), H-5 to 7.64 ppm (dd, J_1 = 5.0, J_2 = 1.2, 1H), and H-4 to 7.13 ppm (dd, J_1 = 5.0, J_2 = 3.8, 1H).

For the signal assignment of 2-methyl thiophene (**2c**; Figure 7), the methyl proton situates at 2.62 ppm (d, J = 1.2 Hz, 3H). By selective decoupling of these protons, the coupling with H-3 disappears. Therefore, H-3 can be assigned to 6.89 ppm (m, 1H). H-4 can then be assigned to 7.02 ppm (dd, J_1 = 5.2 Hz, J_2 = 3.4 Hz, 1H), and H-5 appears at 7.19 ppm (dd, J_1 = 5.2 Hz, J_2 = 1.2 Hz, 1H). The carbon shifts have been assigned by APT and HETCOR.

Figure 7. Assignment of the chemical shifts of 2-methyl thiophene (**2c**).

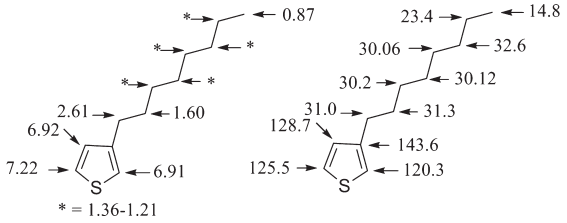

Figure 8. Assignment of the chemical shifts of 3-octyl thiophene (**2d**).

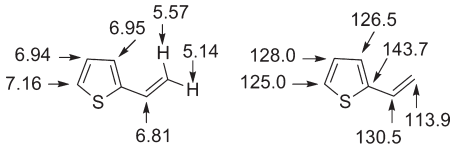

Figure 9. Assignment of the chemical shifts of 2-vinylthiophene (**2e**).

As an intermediate conclusion, it can be stated that for 2-substituted thiophenes the $^3J_{H5-H4}$ coupling is always larger than the $^3J_{H3-H4}$ coupling, thereby providing a useful criterion for signal assignment in this type of compounds.

To achieve the chemical shift information of 3-octylthiophene (**2d**; Figure 8), a somewhat more extensive study was necessary. First, the methylene protons of the side chain closest to the thiophene ring (at δ = 2.61 ppm) were selectively irradiated. This results in the disappearance of the coupling with H-2 and H-4, resulting in the assignment of H5 at 7.22 ppm (dd, J_1 = 4.9 Hz, J_2 = 3.1 Hz, 1H). The corresponding carbon shift can be assigned by HETCOR. C3 is the only quaternary carbon in the structure, so this can be assigned by APT at 143.6 ppm. Starting from C3 or C5, C2 and C4 were further assigned via INADEQUATE to the signals at 120.3 ppm and 128.7 ppm respectively. The corresponding proton shifts were determined by HETCOR [H2: 6.91 ppm (dd, J_1 = 3.1 Hz, J_2 = 1.3 Hz, 1H), H4: 6.92 ppm (dd, J_1 = 4.9 Hz, J_2 = 1.3 Hz, 1H)]. Also the carbon atoms of the alkyl side chain were assigned on the basis of the INADEQUATE experiment. By this all the carbon atoms are determined and the corresponding proton shifts are assigned by HETCOR.

For 2-vinylthiophene (**2e**; Figure 9), the quaternary and CH_2 carbon atoms can be assigned by APT. When two of the six carbon atoms are known, the other four can be derived from the INADEQUATE 2D-spectrum. The corresponding protons were determined by HETCOR.

To retrieve the chemical shifts assignment of the model compound **1d** (Figure 10), the quaternary carbon atom has first been assigned by means of APT (143 ppm). Furthermore, the protons from the double bond are easy to recognize, because they

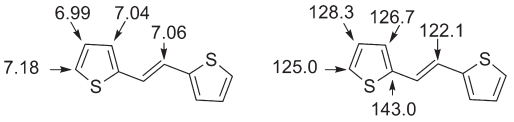

Figure 10. Assignment of the chemical shifts of model compound **1d**.

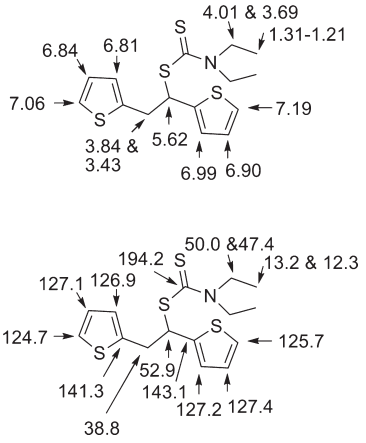

Figure 11. Assignment of the chemical shifts of model compound **1b**.

are the only protons that are represented by a singlet (7.06 ppm). The aromatic protons are assigned based on their coupling constants and all the according carbon atoms are determined by the HETCOR spectrum.

The determination of the chemical shifts of model compound **1b** (Figure 11) was more complicated. First the quaternary, methylene, and methyl carbon atoms have been determined by APT. The quaternary carbon atom of the dithiocarbamate group appears at 194.2 ppm. The quaternary carbon atoms of the aromatic rings have been determined at 143.1 and 141.3 ppm. The chemical shifts at 50.0 and 47.4 ppm arise from the methylene carbon atoms next to the nitrogen atom of the dithiocarbamate group (hindered rotation around the N−C═S bond). The signal at 38.8 ppm corresponds to the bridging methylene group. The remaining aliphatic CH signal at 52.9 ppm can hence be assigned to the bridge methine carbon atom, and the two CH_3 signals at 12.3 and 13.2 ppm arise from the dithiocarbamate group. All the corresponding proton shifts have been determined via the HETCOR spectrum. Finally, all of the aromatic signals had to be assigned. First the proton coupling constants were determined allowing these protons to be positioned on the thiophene rings. For the signal assignment of the protons to the appropriate thiophene rings, a homonuclear $^1H-^1H$ NOE experiment has been performed (selective proton irradiation at 5.62 ppm results in a clear NOE effect at 6.99 ppm). The corresponding carbon signals have been assigned by HETCOR. Finally, the quaternary carbon atoms have been assigned by means of a long-range 2D HETCOR experiment (based on the $^2J_{C-H}$ and $^3J_{C-H}$ couplings between the quaternary carbon atoms and the assigned H-2 and H-3 protons).

For the signal assignment of model compound **1c** (Figure 12), an APT spectrum was first recorded allowing the quaternary and CH_2 carbon atoms to be assigned to 144.3 and 32.8 ppm, respectively. Furthermore, the aromatic protons were assigned by means of their coupling constants. The central proton on the ring was found at 6.93 ppm with coupling constants of 5.1 and 3.6 Hz. The position of the other protons was determined via the

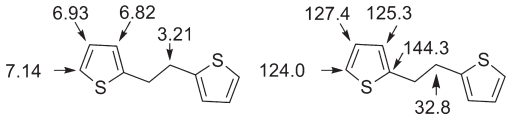

Figure 12. Assignment of the chemical shifts of model compound **1c**.

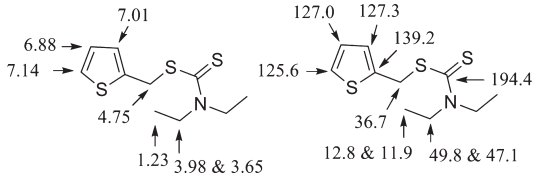

Figure 13. Assignment of the chemical shifts of reference compound **2a**.

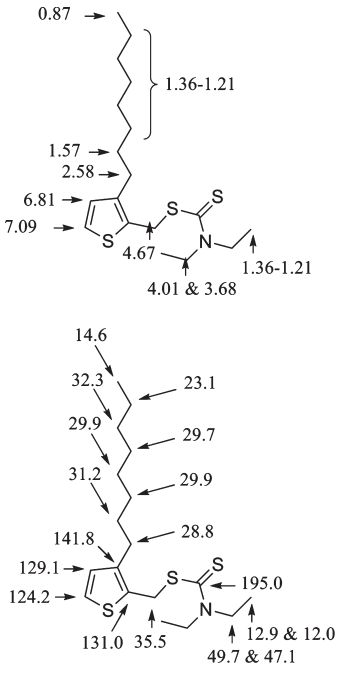

Figure 14. Assignment of the chemical shifts of reference compound **2b**.

J-coupling (H-3: $J_1 = 3.6$ Hz and H-5: $J_1 = 5.1$ Hz) and confirmed by means of long-range HETCOR. A $^2J_{C-H}$ coupling between the quaternary carbon atom at 144.3 ppm and the proton at 6.82 ppm was observed. The corresponding carbon and proton signals have been assigned by means of HETCOR.

For reference compound **2a** (Figure 13) the signal assignment has also been started with APT to assign the quaternary carbon atoms. The aliphatic protons and carbon atoms can be assigned based on their chemical shift and HETCOR information. This leaves only the aromatic protons and carbon atoms. Also here, the coupling constants are very helpful: H-4 can be assigned to the signal at 6.88 ppm based on coupling constants of 5.1 and 3.5 Hz, H-3 ($J_1 = 3.5$ Hz) and H-5 ($J_1 = 5.1$ Hz) to signals at 7.01 and 7.14 ppm, respectively. Again, the assignment of H-3 was confirmed by means of a long-range HETCOR.

For the determination of the chemical shift of reference compound **2b** (Figure 14), the same strategy as for reference compound **2a** was followed, for which all of the aliphatic protons/carbon atoms, except for the octyl tail, were determined. For the assignment of the signals of the octyl tail and the

dithiocarbamate group, the chemical shifts have been compared with those of reference compounds **2d** and **2a**, respectively. In the following step, the two aromatic quaternary carbon atoms were assigned by heteronuclear $^{1}H-^{13}C$ NOE experiments (selective proton irradiation at 4.67 ppm results in a clear NOE for the carbon signal at 131.0 ppm). Finally, the other two aromatic signals have been assigned by means of homonuclear $^{1}H-^{1}H$ NOE experiments (selective proton irradiation at 2.58 ppm results in a NOE effect for the proton signal at 6.81 ppm).

DFT Calculations of the NMR Chemical Shifts of Model and Reference Compounds and Comparison to the Experiment. Figure 15a−f compare the experimental and theoretical chemical shifts collected in Table S1 for the reference compounds and model compounds **1b**−**d** and provide a hierarchy of

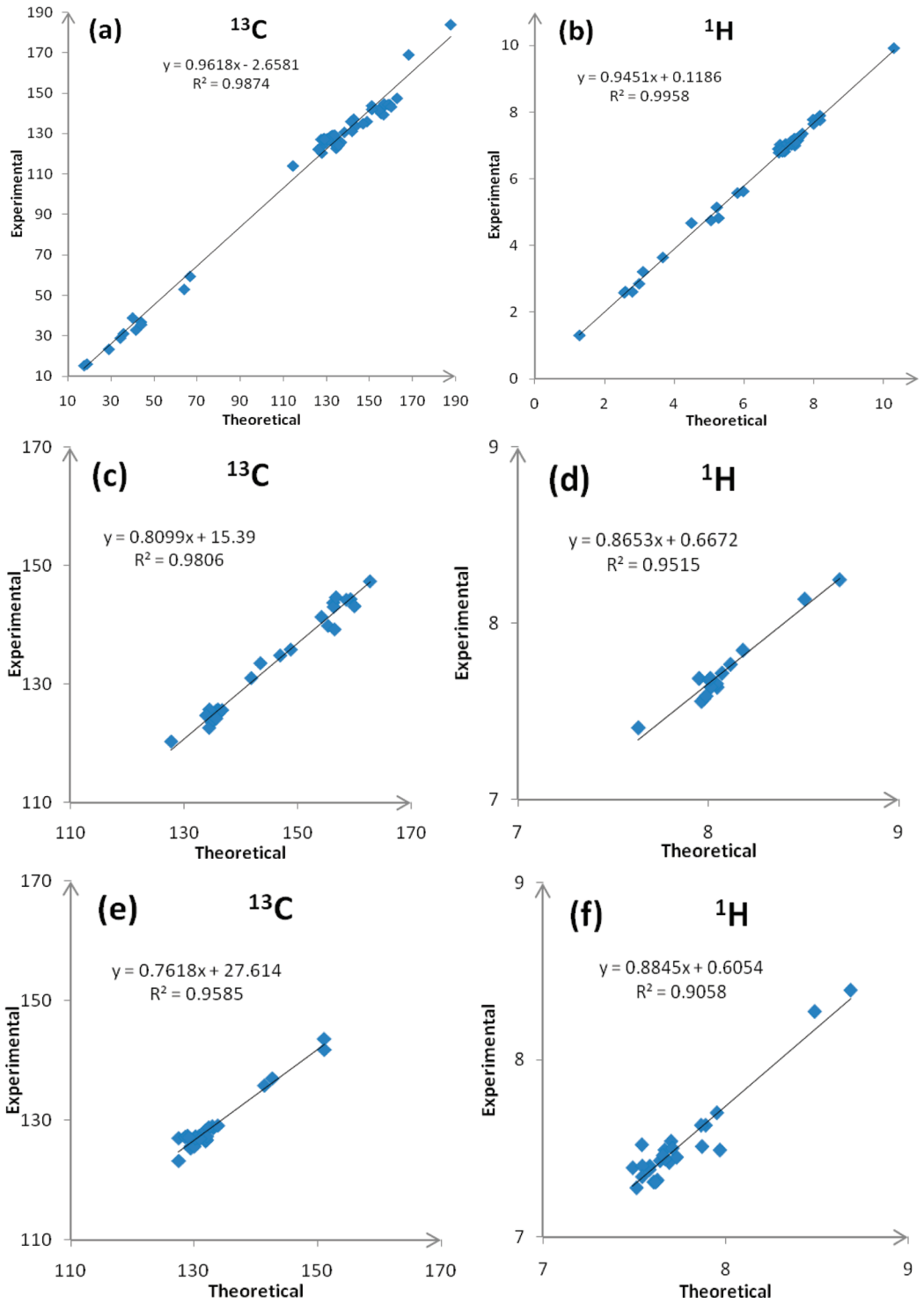

Figure 15. Linear regressions between the experimental and the B3LYP/6-311+G(2d,p) chemical shifts (in ppm); (a) all sp^2 and sp^3 hybridized C atoms and (b) their linked H atoms; (c) α sp^2 hybridized C atoms and (d) their linked H atoms; (e) β sp^2 hybridized C atoms and (f) their linked H atoms.

dx.doi.org/10.1021/jp206663v |J. Phys. Chem. B 2011, 115, 12040–12050

linear regressions. All of the sp^3 and sp^2 carbon atoms and the linked hydrogen atoms were considered in Figure 15, panels a and b. Linear regressions are characterized by rather large R^2 values and a substantial reduction of the mean absolute errors (MAE). Indeed, a direct comparison between the calculated and the experimental chemical shifts yields MAE of 7.31 and 0.26 ppm for the ^{13}C and ^{1}H chemical shifts, while, after correcting the δ values using the linear regression, the corrected MAE (CMAE) shrink to 3.83 and 0.08 ppm, respectively. Nevertheless, a single equation for correcting all C or all H turns out to be insufficient. This is substantiated by comparing the so-corrected chemical shifts to the experimental values: the ^{13}C δ values are almost systematically overestimated for the C atoms in positions 2, 5, and 6, whereas for those in positions 3 and 4, they are underestimated. Therefore, in several cases, this leads to an inversion of the predicted C_4 versus C_5 (C_2 versus C_3) chemical shifts with respect to the experiment. Calculations carried out for thiophene at the second-order Møller−Plesset (MP2) level (for determining both the ground-state geometry and the shielding constants) demonstrate that these systematic errors are related to subtle electron correlation effects, which are not grasped by the B3LYP and BHandHLYP functionals. In fact, the difference of the chemical shifts between C_2 and C_3 goes from 5.01 ppm with B3LYP (BHandHLYP) to 0.34 ppm when employing MP2, which nicely improves the agreement with the experimental values for thiophene.

Therefore, in a second step, we have taken into account the different hybridizations for the C atoms and the linked H atoms in the linear regressions. The most satisfactory approach — leading to the best δ estimates — distinguishes between the thiophene ring atoms (sp^2 C atoms and the H atoms linked to these) and the others, but most importantly, the former ones are separated into the atoms in α positions (2 and 5) and those in β positions (3 and 4). The corresponding figures and linear regressions are provided in Figure 15, panels c and d (α positions) and panels e and f (β positions). Due to the narrower range of chemical shift variations, the R^2 values are smaller than when considering the whole set of C and H atoms but the remaining MAE are smaller: the CMAE amounts to 2.09 ppm for ^{13}C and 0.07 ppm for ^{1}H. In such a case, the relative shieldings at the α and β positions are correctly predicted. To summarize, the best agreement with experiment is obtained when (i) the δ values in α and β positions are extracted from the linear fit equations given in Figure 15c−f, whereas (ii) the fits of Figure 15, panels a and b, are used for the other atoms. This leads to global CMAE of 1.43 and 0.06 ppm for ^{13}C and ^{1}H chemical shifts, respectively.

The key quantities for analyzing the data and assigning the chemical shifts are, however, the variations in the chemical shifts induced by grafting different substituents on the thiophene ring. These values, listed in Table 1, provide specific signatures for the different chemical groups. Overall, the experimental trends are well reproduced in both amplitude and sign by the DFT calculations, in particular for the ^{1}H chemical shifts. More particularly, it is worth mentioning that (i) the deshielding (shielding) is stronger on C_6 (H_6) for the compound (**2e**) than for the dimer (**1d**), which contain both a vinyl substituent, and (ii) upon substitutions in positions 2 and 3, a shielding is observed for H_3, H_4 and H_5 as well as a deshielding for H_6, with the exception of cases where the substituent is a mesomeric attracting group.

DFT Calculations of the NMR Chemical Shifts of Model Compounds that Are not Experimentally Available. Simulated chemical shifts of structures **1a**, **1e**, and **1f** are displayed in

Table 1. Variations (Δ, in ppm) of the Calculated Chemical Shifts with Respect to Reference Compounds[a]

		^{13}C				^{1}H		
		method 1	method 2	exp.		method 1	method 2	exp.
2c	C_2	19.33	15.66	14.10				
	C_3	−1.66	−1.26	−1.80	H_3	−0.40	−0.35	−0.24
	C_4	−0.85	−0.65	−0.10	H_4	−0.35	−0.31	−0.11
	C_5	−1.11	−0.90	−2.20	H_5	−0.23	−0.20	−0.16
2c*	C_2	26.70	21.62	21.60				
	C_3	−3.60	−2.75	−4.20	H_3	−0.38	−0.34	−0.35
	C_4	−0.77	−0.59	−0.80	H_4	−0.31	−0.27	−0.23
	C_5	−1.56	−1.26	−3.10	H_5	−0.20	−0.18	−0.27
	C_6	11.50	11.06	8.10	H_6	0.40	0.38	0.23
2d	C_2	−8.22	−6.66	−5.40	H_2	−0.55	−0.48	−0.44
	C_3	19.96	15.21	16.20				
	C_4	2.03	1.55	1.30	H_4	−0.20	−0.18	−0.21
	C_5	−0.34	−0.28	−0.20	H_5	−0.11	−0.10	−0.13
2e	C_2	20.26	16.41	18.00				
	C_3	0.76	0.58	−0.90	H_3	−0.16	−0.14	−0.18
	C_4	0.55	0.42	0.60	H_4	−0.22	−0.20	−0.19
	C_5	0.08	0.06	−0.70	H_5	−0.14	−0.12	−0.19
	C_6	120.96	116.34	115.30	H_6	4.57	4.32	4.19
2f	C_2	20.73	16.79	18.90				
	C_3	11.58	8.82	9.60	H_3	0.60	0.53	0.64
	C_4	1.86	1.42	1.60	H_4	0.06	0.05	0.07
	C_5	12.77	10.34	10.10	H_5	0.51	0.44	0.40
	C_6	170.35	163.84	168.50	H_6	7.71	7.28	7.29
2g	C_2	22.56	18.27	18.50				
	C_3	−3.60	−2.74	−0.40	H_3	−0.18	−0.16	−0.13
	C_4	−1.08	−0.82	−1.80	H_4	−0.23	−0.21	−0.17
	C_5	0.16	0.13	−0.20	H_5	−0.07	−0.06	−0.08
	C_6	49.21	47.33	44.10	H_6	2.68	2.53	2.20
2h	C_2	7.45	6.03	7.80				
	C_3	10.30	7.84	8.40	H_3	0.79	0.70	0.76
	C_4	1.26	0.96	1.40	H_4	−0.03	−0.02	0.00
	C_5	10.92	8.84	9.10	H_5	0.33	0.28	0.29
	C_6	150.85	145.08	153.60	H_6	−2.60	−2.58	−2.62
2a	C_2	20.48	16.58	13.50				
	C_3	0.95	0.73	−0.10	H_3	−0.02	−0.02	−0.12
	C_4	−0.84	−0.64	−0.40	H_4	−0.31	−0.27	−0.25
	C_5	0.71	0.57	−0.10	H_5	−0.17	−0.15	−0.21
	C_6	26.45	25.44	21.50	H_6	2.46	2.32	2.13
2b	C_2	5.84	4.73	5.30				
	C_3	20.01	15.24	14.40				
	C_4	2.74	2.09	1.70	H_4	−0.28	−0.24	−0.32
	C_5	−0.33	−0.26	−1.50	H_5	−0.19	−0.17	−0.26
	C_6	26.54	25.53	20.30	H_6	1.90	1.79	2.05
1b	C_2	23.97	19.41	17.40				
	C_3	−2.55	−1.95	−0.20	H_3	0.08	0.07	−0.14
	C_4	−2.18	−1.66	0.00	H_4	−0.35	−0.31	−0.23
	C_5	−1.52	−1.23	0.00	H_5	−0.17	−0.15	−0.16
	C_6	46.49	44.71	37.70	H_6	3.39	3.20	3.00
	C_2'	18.18	14.72	15.60				
	C_3'	−0.16	−0.12	−0.50	H_3	−0.29	−0.25	−0.32
	C_4'	−1.95	−1.49	−0.30	H_4	−0.35	−0.31	−0.29
	C_5'	−2.07	−1.67	−1.00	H_5	−0.22	−0.19	−0.29

dx.doi.org/10.1021/jp206663v |J. Phys. Chem. B 2011, 115, 12040–12050

Table 1. Continued

		^{13}C			^{1}H			
		method 1	method 2	exp.		method 1	method 2	exp.
	C_6'	22.53	21.67	23.60	H_6	1.08	1.02	1.02
1c	C_2	23.29	18.86	18.60				
	C_3	−1.66	−1.27	−2.10	H_3	−0.27	−0.23	−0.31
	C_4	−0.23	−0.18	0.00	H_4	−0.25	−0.22	−0.20
	C_5	−0.92	−0.75	−1.70	H_5	−0.14	−0.12	−0.21
	C_6	24.06	23.14	17.60	H_6	0.51	0.48	0.59
1d	C_2	20.33	16.47	17.30				
	C_3	0.94	0.72	−0.70	H_3	−0.19	−0.17	−0.09
	C_4	0.74	0.56	0.90	H_4	−0.22	−0.20	−0.14
	C_5	−0.61	−0.50	−0.70	H_5	−0.18	−0.15	−0.17
	C_6	108.87	104.72	106.90	H_6	4.76	4.50	4.44
MAE/ CMAE		**7.31**	**1.43**			**0.26**	**0.06**	

[a] For C_2−C_5, $\Delta = \delta_{\text{substituted thiophene}} - \delta_{\text{thiophene}}$, whereas for C_6, $\Delta = \delta_{\text{substituted thiophene}} - \delta_{\text{2-methylthiophene}}$. In method 1, the chemical shifts are not corrected for systematic errors, though the MB weights are considered for the different conformers. In method 2, in addition to MB averaging, the chemical shifts are corrected. For atoms 2 and 5, (c) and (d) fittings (Figure 15) were employed. The (e) and (f) fittings are used for atoms 3 and 4 while for atom 6, the (a) and (b) fitting were applied. **2c*** = 2-ethylthiophene; Experimental data from [Spectral Database SDBS http://riodb01.ibase.aist.go.jp/sdbs/cgi-bin/direct_frame_top.cgi].

Table 2 so as to assist in the interpretation of the O-PTV polymerization process. For the first two species (**1a**, **1e**), two conformers contribute to the MB-averaged results while only one conformer is relevant for **1f**. For these three compounds the best δ estimates, obtained as described above by using different linear regression corrections for different types of atoms, are reported. Table 2 also displays the differences between these δ values and those of the thiophene and 2-methylthiophene reference compounds. Comparing the $\Delta(\delta)$ of **1a**, **1e**, and **1f** with those of Table 1, clear fingerprints can be identified, including (i) the obvious deshielding of the DTC-substituted C_6 (**1a** versus **1b** and **1c** or **1e** versus **1d**) or shielding of the triple bond C_6 in **1f**, and (ii) the impact on the DTC substitution on the thiophene ring atoms as evidenced by the deshielding of C_3 in **1a** with respect to **1b** and **1c**, the deshielding of C_3' and C_5' in **1e** with respect to **1d**, as well as the shielding of C_2 and the deshielding of C_3 and C_5 in **1f** with respect to **1d**.

The chemical shift information gathered from Table 2 can be used to identify/confirm the structural defects in the polymer backbone of (precursor) O-PTV.[37] The calculated chemical shift (60.98 ppm) for C6 of model compound **1a** is in good agreement with the chemical shift assignment at 58.2 ppm of the tail-to-tail defect structure identified in the experimental ^{13}C NMR spectrum of the labeled precursor polymer.[37] For model compound **1f** a characteristic chemical shift of 89.52 ppm has been determined for the triple bond. In this region, no signals are present in the NMR spectrum indicating that no full elimination of the tail-to-tail defects occur within the NMR detection limit. A single elimination however, represented by model compound **1e**, cannot be excluded since the carbon signals of the double bonds (at 123.4 and 131.5 ppm) would end up in the huge massif (100−150 ppm) of the ^{13}C-labeled olefinic carbon atoms.

Table 2. Calculated Chemical Shifts (Using Method 2) and Differences of Chemical Shifts with Respect to Thiophene and 2-Methylthiophene (for C_6 and H_6) in ppm for Compounds 1a, 1e, and 1f

		δ	$\Delta(\delta)$		δ	$\Delta(\delta)$
1a	C_2	145.01	19.43			
	C_3	127.85	0.39	H_3	7.33	0.18
	C_4	126.69	−0.77	H_4	6.83	−0.32
	C_5	125.66	0.07	H_5	7.16	−0.15
	C_6	60.98	46.96	H_6	6.17	3.60
1e	C_2	146.73	21.14			
	C_3	127.21	−0.26	H_3	7.22	0.08
	C_4	127.81	0.35	H_4	6.94	−0.20
	C_5	125.53	−0.05	H_5	7.17	−0.14
	C_6	123.42	109.40			
	C_2'	138.97	13.38			
	C_3'	133.48	6.02	H_3'	7.25	0.11
	C_4'	126.93	−0.53	H_4'	7.01	−0.13
	C_5'	130.02	4.44	H_5'	7.37	0.05
	C_6'	131.53	117.51	H_6'	7.61	5.04
1f	C_2	125.29	−0.29			
	C_3	132.13	4.67	H_3	7.24	0.10
	C_4	127.99	0.53	H_4	6.96	−0.18
	C_5	127.74	2.15	H_5	7.21	−0.10
	C_6	89.52	75.50			

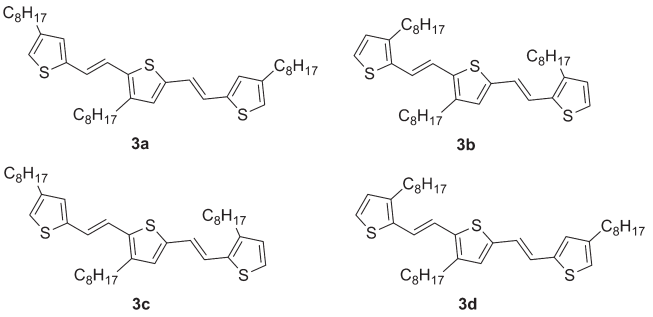

Figure 16. Different model compounds to study the regioregularity of O-PTV.

REGIOREGULARITY

In the literature, it is claimed on the basis of ^{1}H and ^{13}C NMR spectroscopy that poly(thienylene vinylene) derivatives, which are prepared via a condensation reaction, are 100% regioregular.[21,38] In order to find criteria to determine the regioregularity of O-PTV, this joint experimental-theoretical NMR study also tackles the determination of the chemical shifts of the following four model compounds (Figure 16) to estimate whether their synthesis is worthwhile and whether NMR is suitable to describe the degree of regioregularity. These model compounds represent the different regioregularity patterns that can occur in experimentally synthesized PTV derivatives.

For each of the isomers **3a**−**3d** (see Figure 17 for clarification of the atom numbering), Table S4 lists the NMR data of all conformers, the MB distribution weights, and the weighted chemical shifts, which also account for the corrections of the systematic errors obtained using the linear regression parameters determined above. One or two conformers account for most of

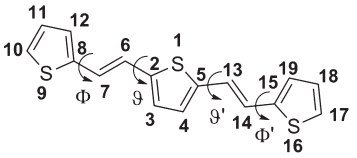

Figure 17. Characteristic dihedral angles $S_1-C_2-C_6-C_7$ (θ), $S_1-C_5-C_{13}-C_{14}$ (θ'), $S_9-C_8-C_7-C_6$ (ϕ), and $S_{16}-C_{15}-C_{14}-C_{13}$ (ϕ'). The atom numbering follows Table 3.

the MB distribution: 40% and 37%, 59% and 25%, 97%, and 63%, and 21% for the isomers **3a**, **3b**, **3c**, and **3d**, respectively. The different conformations are displayed in Figure S2. All characteristic backbone dihedral angles are close to 0° or 180°, except for the D conformer of **3b**, where ϕ' amounts to 163°. These most stable structures correspond to conformations where two or three alkyl chains linked to consecutive thiophene rings closely interact, as a result of stabilizing van der Waals forces. As a consequence the corresponding S atoms point toward the same direction. Such conformations are driven by the dispersion correction of the B97-D functional.

For the sake of comparison between the different isomers, Table 3 lists selected chemical shifts and chemical shift differences for isomers **3a**, **3b**, **3c**, and **3d**. These data highlight several signatures of the regioregular product **3c**, for which the prominence of a single stable conformer displays a maximum of interactions between the three alkyl chains. In particular, the C_6 (C_7) and C_{13} (C_{14}) atoms are more deshielded (shielded) than in the other isomers, in addition to the strong deshielding of H_6. Other remarkable differences in ^{1}H chemical shifts are the deshielding of H_4 and H_{14} in **3b**. This deshielding of H_4 in **3b**, with respect to thiophene as well as to **2d** and **2e**, that bear the same type of substituents, contrasts with the small deshielding calculated for **3a**, **3c**, and **3d**. This suggests that the conformational effect is crucial. Indeed, the most stable conformer of **3b**, contributing to about 60% of the MB distribution, presents a $\theta' \approx 180°$ [$\delta(H_4) = 7.65$ ppm], whereas a clearly different value $\delta(H_4) \approx 6.85$ ppm is encountered for conformations A and B of **3a**, C of **3b**, A of **3c**, as well as A and B of **3d**, where the angle θ' is always around 0°. This analysis is also confirmed by the slight shielding undergone by C_4 of **3b** (129.8 ppm) and the corresponding considerable deshielding in **3a**, **3c** and **3d** compared with **2d** (132.8 ppm, 133.0 ppm and 132.6 ppm versus 129.0 ppm).

Among the remarkable δ differences, the $\delta(C_5) - \delta(C_2)$ quantity attains 4.71 ppm for **3c** but reduces to 4.07, 3.86, and 3.50 ppm for **3a**, **3b**, and **3d**, respectively. On the other hand, the $\delta(C_3) - \delta(C_4)$ difference amounts to 13.0, 11.2, 10.8, and 9.4 ppm for **3b**, **3c**, **3a**, and **3d**, respectively. Besides $\delta(C_3) - \delta(C_4)$, the largest values among these differences of chemical shifts between pairs of C or H atoms are always coming from **3c** even though some other clear differences can be pointed out, encompassing $[\delta(C_{15}) - \delta(C_8)] = 5.52$ ppm and $[\delta(C_{17}) - \delta(C_{10})] = -3.66$ ppm in **3d**, $[\delta(H_{13}) - \delta(H_6)] = -0.33$ ppm in **3a**, $[\delta(H_{14}) - \delta(H_7)] = 0.30$ ppm in **3b**, and $[\delta(H_{17}) - \delta(H_{10})] = -0.31$ ppm in **3d**. Moreover, the largest $\delta(H_{13}) - \delta(H_6)$ and $\delta(H_{14}) - \delta(H_7)$ differences are also obtained for **3c** (−0.83 and 0.34 ppm), providing other signatures of the regioregular substitution pattern.

All of these differences result from the change in the relative substitution patterns and thereof from the change of conformations steered by the relative position of the alkyl chains. Indeed, the most stable conformers (two for **3a**, **3b**, and **3d** and only one for **3c**) are essentially not the same for the different configurations, leading to specific contributions to the δ's. To confirm these theoretical calculations it would be useful to synthezise the model compounds **3a**−**3d**.

However, the trimers are no explicit models for regioregular polymers since C_{10} and C_{17} will then no longer be methine carbon atoms. For longer, fully regioregular oligomers and polymers, one would expect only one chemical shift for C_6 and C_{14} as well as for C_7 and C_{13}. However, based on the theoretical calculations, it can be expected that any change in the regioregularity will induce geometrical and conformational changes, leading to the observation of more than two chemical shifts for the olefinic carbon atoms. Therefore, it can be concluded that ^{13}C NMR should be able to detect significant deviations from regioregularity.

Table 3. Calculated Chemical Shift and Their Differences for Structures 3a, 3b, 3c, and 3d Obtained after Maxwell−Boltzmann Averaging and after Correcting the Chemical Shifts with the Linear Regression Parameters Determined before[a]

	3a		3b		3c		3d	
$\delta(C_2)$	138.03	*-3.96*	138.12	*-3.87*	137.89	*-4.10*	137.22	*-4.77*
$\delta(C_3)$	143.59	*15.55*	142.82	*14.78*	144.14	*16.10*	142.01	*13.97*
$\delta(C_4)$	132.84	*4.96*	129.83	*1.95*	132.95	*5.07*	132.60	*4.72*
$\delta(C_5)$	142.10	*16.45*	141.98	*16.33*	142.60	*16.95*	140.72	*15.07*
$\delta(C_6)$	119.95	*-10.41*	118.75	*-11.61*	120.29	*-10.07*	117.74	*-12.62*
$\delta(C_7)$	121.34	*-9.02*	120.21	*-10.15*	115.41	*-14.95*	119.12	*-11.24*
$\delta(C_8)$	144.93	*2.94*	139.39	*-2.60*	144.68	*2.69*	138.20	*-3.79*
$\delta(C_{10})$	122.45	*-3.20*	126.23	*0.58*	121.69	*-3.96*	125.46	*-0.19*
$\delta(C_{13})$	119.94	*-10.42*	119.71	*-10.65*	124.31	*-6.05*	118.77	*-11.59*
$\delta(C_{14})$	120.74	*-9.62*	119.98	*-10.38*	119.33	*-11.03*	119.67	*-10.69*
$\delta(C_{15})$	134.36	*-7.63*	138.38	*-3.61*	139.12	*-2.87*	143.72	*1.73*
$\delta(C_{17})$	120.43	*-5.22*	126.87	*1.22*	126.84	*1.19*	121.80	*-3.85*
$\delta(H_4)$	6.89	*-0.06*	7.37	*0.42*	6.85	*-0.10*	6.88	*-0.07*
$\delta(H_6)$	7.32	*0.42*	7.06	*0.16*	7.64	*0.74*	6.98	*0.08*
$\delta(H_7)$	6.90	*0.00*	7.13	*0.23*	6.65	*-0.25*	7.06	*0.16*
$\delta(H_{10})$	6.94	*-0.25*	7.32	*0.13*	6.97	*-0.22*	7.25	*0.06*
$\delta(H_{13})$	6.99	*0.09*	6.85	*-0.05*	6.81	*-0.09*	7.01	*0.11*
$\delta(H_{14})$	7.14	*0.24*	7.43	*0.53*	7.00	*0.10*	7.01	*0.11*
$\delta(H_{17})$	7.00	*-0.19*	7.27	*0.08*	7.29	*0.10*	6.93	*-0.26*
$\delta(C_5) - \delta(C_2)$	4.07		3.86		4.71		3.50	
$\delta(C_3) - \delta(C_4)$	10.75		12.99		11.19		9.41	
$\delta(C_{13}) - \delta(C_6)$	−0.01		0.96		4.02		1.03	
$\delta(C_{14}) - \delta(C_7)$	−0.59		−0.22		3.92		0.55	
$\delta(C_{15}) - \delta(C_8)$	0.08		−1.01		−5.57		5.52	
$\delta(C_{17}) - \delta(C_{10})$	0.50		0.64		5.14		−3.66	
$\delta(H_{13}) - \delta(H_6)$	−0.33		−0.21		−0.83		0.03	
$\delta(H_{14}) - \delta(H_7)$	0.23		0.30		0.34		−0.05	
$\delta(H_{17}) - \delta(H_{10})$	0.06		−0.05		0.32		−0.31	

[a] Values in italics are the differences of the chemical shifts with respect to 2-vinylthiophene (**2e**).

CONCLUSIONS

In this joint experimental−theoretical work, several reference and model compounds are discussed, which have been

synthesized and fully characterized by different NMR techniques in order to obtain chemical shift information regarding the identity of structural defects and regioregularity in PTV-based polymers. Among others, it has been noticed that for 2-substituted thiophenes the $^3J_{H5-H4}$ coupling is always larger than the $^3J_{H3-H4}$ coupling and offers a possible fingerprint for NMR assignment. The obtained chemical shift information has been used to calculate the chemical shifts of several other model compounds. This information is useful to verify the structural defects on the polymer level and to determine the degree of regioregularity of the polymers. Furthermore, the experimental NMR results can be used to further refine chemical shift prediction software.

■ ASSOCIATED CONTENT

Supporting Information. Calculated results at the IEFPCM($CHCl_3$)/B3LYP/6-311+G(2d,p) level corrected using different linear regressions [all sp^3 and sp^2 atoms (Table S1), all sp^2, α sp^2, and β sp^2 atoms (Table S2)]. Linear regressions using all sp^2 as well as α and β sp^2 carbon atoms and attached hydrogen atoms (Figure S1). Calculated results at IEFPCM(CHCl3)-B3LYP/6-311+G(2d,p) with the most appropriate correction using linear regression (Table S3). Most stable conformers obtained with B97-D for configurations **3a**, **3b**, **3c**, and **3d** (Figure S2). Chemical shifts for the most stable conformers calculated using B97-D functional for configurations **3a, 3b, 3c**, and **3d** (Table S4). This material is available free of charge via the Internet at http://pubs.acs.org.

■ AUTHOR INFORMATION

Corresponding Author

*Phone +32 (0) 11 268396. E-mail: peter.adriaensens@uhasselt.be.

■ ACKNOWLEDGMENT

We gratefully acknowledge BELSPO in the frame of the IAP P6/27 network, and the IWT (Institute for the Promotion of Innovation by Science and Technology in Flanders) for the financial support via the SBO-project 060843 'PolySpec'. We also want to thank the EU for the FP6-Marie Curie-RTN 'SolarNtype' (MRTN-CT-2006-035533). Furthermore, the support of the Fund for Scientific Research-Flanders (FWO projects G.0161.03N, G.0252.04N, and G.0091.07N) is acknowledged. The calculations were performed on the Interuniversity Scientific Computing Facility (ISCF) installed at the Facultés Universitaires Notre-Dame de la Paix (FUNDP, Namur, Belgium), for which we gratefully acknowledge financial support from the FRS-FRFC (Convention No. 2.4.617.07.F), and FUNDP. Research in Mons is also supported by FEDER (SMARTFILM project) and the Région Wallonne (OPTI2MAT excellence program). D.B. is FNRS Research Director.

■ REFERENCES

(1) Horowitz, G. *Adv. Mater.* **1998**, *10*, 365–377.
(2) Gerard, M.; Chaubey, A.; Malhotra, B. D. *Biosens. Bioelectron.* **2002**, *17*, 345–359.
(3) Burroughes, J. H.; Bradley, D. D. C.; Brown, A; Marks, R. N.; Mackay, K; Friend, R. H.; Burns, P. L.; Holmes, A. B. *Nature* **1990**, *347*, 539–541.
(4) Spanggaard, H.; Sariciftci, F. C. *Sol. Enery Mater. Sol. Cells* **2004**, *83*, 125–146.
(5) Sariciftci, N. S. *Mater. Today* **2004**, 36–40.
(6) de Boer, B.; Facchetti, A. *Polym. Rev.* **2008**, *48*, 423–431.
(7) Dhanabalan, A.; van Duren, J. K. J.; van Hal, P. A.; van Dongen, J. L. J.; Janssen, R. A. J. *Adv. Funct. Mater.* **2001**, *11*, 255–262.
(8) Bundgaard, E.; Krebs, F. C. *Sol. Enery Mater. Sol. Cells* **2007**, *91*, 954–985.
(9) Kroon, R.; Lenes, M.; Hummelen, J. C.; Blom, P. W. M.; de Boer, B. *Polym. Rev.* **2008**, *48*, 531–582.
(10) Winder, C.; Sariciftci, N. S. *J. Mater. Chem.* **2004**, *14*, 1077–1086.
(11) Goris, L.; Loi, M. A.; Cravino, A.; Neugebauer, H.; Sariciftci, N. S.; Polec, I.; Lutsen, L.; Manca, J.; De Schepper, L.; Vanderzande, D. *Synth. Met.* **2003**, *138*, 249–253.
(12) Colladet, K.; Nicolas, M.; Goris, L.; Lutsen, L.; Vanderzande, D. *Thin Solid Films* **2004**, *7*, 451–452.
(13) Shaheen, S. E.; Vangeneugden, D.; Kiebooms, R.; Vanderzande, D.; Fromherz, T.; Padinger, F.; Brabec, D. J.; Sariciftci, N. S. *Synth. Met.* **2001**, *121*, 1583–1584.
(14) Gravilenko, A. V.; Matos, T. D.; Bonner, B. E.; Sun, S.-S.; Zhang, C.; Gravilenko, V. I. *J. Phys. Chem.* **2008**, *112*, 7908–7912.
(15) Xie, H.-Q.; Liu, C.-M.; Guo, J.-S. *Eur. Polym. J.* **1996**, *32*, 1131–1137.
(16) Fuchigami, H.; Tsumura, A.; Koezuka, H. *Appl. Phys. Lett.* **1993**, *63*, 1372–1374.
(17) Henckens, A.; Colladet, K.; Fourier, S.; Cleij, T. J.; Lutsen, L.; Gelan, J.; Vanderzande, D. *Macromolecules* **2005**, *38*, 19–26.
(18) Yeon-Beom, L.; Hong-Ku, S.; Seung-Won, K. *Macromol. Rapid Commun.* **2003**, *24*, 522–526.
(19) Smith, A. P.; Smith, R. R.; Taylor, B. E.; Durstock, M. F. *Chem. Mater.* **2004**, *16*, 4687–4692.
(20) Van De Wetering, K.; Brochon, C.; Nhov, C.; Hadziioannou, G. *Macromolecules* **2006**, *39*, 4289–4297.
(21) Loewe, R. S.; McCullough, R. D. *Chem. Mater.* **2000**, *12*, 3214–3221.
(22) Harper, K.; West, W. J. W. Eur. Pat. Appl. No. 182548, 1985.
(23) Jen, K. Y.; Jow, R.; Eckhardt, H.; Elsenbaumer, R. L. *Polym. Mater. Sci. Eng.* **1987**, *56*, 49–53.
(24) Jen, K. Y.; Maxfield, M.; Shacklette, L. W.; Elsenbaumer, R. L. *J. Chem. Soc., Chem. Commun.* **1987**, 309–311.
(25) Yamada, D.; Tokito, S.; H.; Tsutsui, T; Saito, S. *J. Chem. Soc., Chem. Commun.* **1987**, 1448–1449.
(26) Tokito, S; Momii, T.; Murata, H; Tsutsui, T.; Saito, S. *Polymer* **1990**, *31*, 1137–1141.
(27) Tsutsui, T.; Murata, H.; Momii, T.; Yoshiura, K.; Tokito, S.; Saito, S. *Synth. Met.* **1991**, *41*, 327–330.
(28) Murase, I.; Ohnishi, T.; Noguchi, T. Ger. Offen. No. 3704411, 1987.
(29) Henckens, A.; Knipper, M.; Polec, I.; Manca, J.; Lutsen, L.; Vanderzande, D. *Thin solid films* **2004**, *451−452*, 472–579.
(30) Henckens, A. Ph.D. dissertation; University of Hasselt: Diepenbeek, Belgium, 2003.
(31) Mitchell, W. J.; Pena, C.; Burn, P. L. *J. Mater. Chem.* **2002**, *12*, 200–205.
(32) Diliën, H.; Palmaerts, A.; Lenes, M.; de Boer, B.; Blom, P.; Cleij, T. J.; Lutsen, L.; Vanderzande, D. *Macromolecules* **2010**, *43*, 10231–10240.
(33) Henckens, A.; Lutsen, L.; Vanderzande, D.; Knipper, M.; Manca, J. *J. SPIE Proc.* **2004**, 52–59.
(34) Banishoeib, F.; Fourier, S.; Cleij, T. J.; Lutsen, L.; Vanderzande, D. *Eur. Phys. J. Appl. Phys.* **2007**, *37*, 237–240.
(35) Nguyen, L. H.; Günes, S.; Neugebauer, H.; Sariciftci, N. S.; Banishoeib, F.; Henckens, A.; Cleij, T. J.; Lutsen, L.; Vanderzande, D. *Sol. Enery Mater. Sol. Cells* **2006**, *90*, 2815–2828.
(36) Banishoeib, F.; Adriaensens, P.; Berson, S.; Guillerez, S.; Douheret, O.; Manca, J.; Fourier, S.; Cleij, T. J.; Lutsen, L.; Vanderzande, D. *Sol. Enery Mater. Sol. Cells* **2007**, *91*, 1026–1034.

(37) Diliën, H.; Chambon, S.; Cleij, T. J.; Lutsen, L.; Vanderzande, D.; Adriaensens, P. J. *Macromolecules* **2011**, *44*, 4711–4720.
(38) Zhang, C.; Matos, T.; Li, R.; Sun, S.-S.; Lewis, J. E.; Zhang, J.; Jiang, X. *Polym. Chem.* **2010**, 663–669.
(39) d'Antuono, P.; Botek, E.; Champagne, B.; Wieme, J.; Reyniers, M. F.; Marin, G. B.; Adriaensens, P. J.; Gelan, J. *Chem. Phys. Lett.* **2007**, *436*, 388–393.
(40) d'Antuono, Ph.; Botek, E.; Champagne, B.; Wieme, J.; Reyniers, M. F.; Marin, G. B.; Adriaensens, P. J.; Gelan, J. *J. Phys. Chem. B* **2008**, *112*, 14804–14818.
(41) d'Antuono, Ph.; Botek, E.; Champagne, B.; Maton, L.; Taziaux, D.; Habib-Jiwan, J. L. *Theor. Chem. Acc.* **2009**, *125*, 461–470.
(42) Botek, E.; d'Antuono, Ph.; Jacques, A.; Carion, R.; Maton, L.; Taziaux, D.; Habib-Jiwan, J. L. *Phys. Chem. Chem. Phys.* **2010**, *12*, 14172–14187.
(43) Tomasi, J.; Mennucci, B.; Cammi, R. *Chem. Rev.* **2005**, *105*, 2999–3093.
(44) d'Antuono, Ph.; Botek, E.; Champagne, B.; Spassova, M.; Denkova, P. *J. Chem. Phys.* **2006**, *125*, 144309.
(45) Diliën, H.; Vandenbergh, J.; Banishoeb, F.; Adriaensens, P.; Cleij, T. J.; Lutsen, L.; Vanderzande, D. J. M. *Macromolecules* **2011**, *44*, 711–718.